Ann Sci For (1997) 54, 313-333

Original article

Assessment of the spatial distribution of light transmitted below young trees in an agroforestry system

S Meloni [1*], H Sinoquet [2]

[1] *Cemagref, domaine de Laluas, 63200 Riom ;*
[2] *Inra, domaine de Crouelle, 63039 Clermont-Ferrand cedex 02, France*

(Received 15 November 1996; accepted 24 January 1997)

Summary – Transmitted radiation under trees shows variability in space and time that may have implications for the understorey. Light measurements were made in a young agroforestry system to assess the radiation distribution below the tree canopy. Measurements show that the variability of the transmitted radiation is mostly due to the size of the tree shadow and to the irradiance distribution in the shaded area. The light measurements were used to test the predictive capacity of a three-dimensional radiative transfer model based on the turbid medium analogy. The model correctly simulates the fraction of sunlit area and the irradiance distribution in the shaded area. However, it underestimates low radiation values and fails in describing the fine spatial pattern of transmitted radiation because of the stochastic nature of the radiation field. To obtain a mean error less than 15% of the incident radiation, the distribution of transmitted radiation has to be described by elementary soil surface areas over 0.08 m^2.

photosynthetically active radiation / spatial distribution / canopy geometry / agroforestry / *Prunus avium*

Résumé – Répartition spatiale du rayonnement transmis sous de jeunes arbres en système agroforestier. Dans une plantation à large espacement, le rayonnement transmis disponible pour la strate inférieure est très variable dans l'espace et dans le temps. Cette hétérogénéité peut avoir des conséquences sur le fonctionnement de la strate inférieure. Des mesures de rayonnement utile à la photosynthèse ont été effectuées pour étudier la distribution du rayonnement sous les couronnes de jeunes merisiers plantés à faible densité. Ces mesures servent également à valider un modèle de transfert radiatif. Les mesures montrent que la variabilité du rayonnement transmis au niveau de la strate inférieure est essentiellement due à la taille de l'ombrage projeté par les arbres et à la distribution du rayonnement dans la surface ombragée. Le modèle simule correctement la proportion de surface ensoleillée ainsi que la distribution du rayonnement dans la surface ombragée. Cependant, il sous-estime la

* Correspondence and reprints
Tel: (33) 04 73 64 50 81; fax: (33) 04 73 64 50 51

valeur minimale du rayonnement transmis et ne permet pas de simuler sa répartition spatiale à une échelle fine en raison de la nature stochastique du rayonnement transmis. Pour une simulation correcte de la répartition spatiale du rayonnement transmis, la surface minimale de simulation doit être comprise entre 0,08 et 0,18 m^2.

rayonnement photosynthétiquement actif / répartition spatiale / géométrie du couvert / agroforesterie / *Prunus avium*

INTRODUCTION

Agroforestry is defined as a multiple land-use system in which woody plants are combined with annual crops and/or animals on the same unit of land (Jarvis, 1991). In these systems, the tree canopy reduces and modifies the light availability to the understorey, with possible consequences on photosynthesis, water relations and morphogenesis. Previous studies have shown that the mean irradiance under a non-homogeneous canopy may not be a reliable parameter to examine physiological processes because of the non-linear plant responses to light (Baldocchi and Hutchison, 1986; Myneni et al, 1989; Pearcy et al, 1990). For example, the total CO_2 fixed by leaves exposed to brief sunflecks can be 150–200% of the predicted rates from steady-state measurements (Pearcy et al, 1990). The spatial distribution of radiation on the floor is determined by the three-dimensional structure of the overstorey (Chazdon, 1988). In agroforestry systems, the spatial and temporal variability of irradiance is crucial because trees form a real heterogeneous canopy, especially before canopy closure.

A number of radiative transfer models have been applied to agroforestry systems. Geometrical models have been used to calculate the shadows cast by trees described as simple shapes (Quesada et al, 1989; Reid and Ferguson, 1992; Nygren, 1993). Jackson (1983) proposed a general framework to estimate the light available under trees with any shade model. Different types of models based on the turbid medium analogy have been or could be used in agroforestry: McMurtrie and Wolf's model (1983) deals with tree-pasture systems where both strata are assumed to be horizontally homogeneous. Hybrid models combining a geometrical description and the turbid medium theory (eg, Norman and Welles, 1983; Wang and Jarvis, 1990, amongst many others) are able to estimate the radiation transmitted under a tree canopy. Other models abstracting the canopy structure as a set of two- or three-dimensional cells have been applied to trees (Kimes and Kirchner, 1982; Cohen and Fuchs, 1987) or agroforestry (Tournebize and Sinoquet, 1995). All these models were used to simulate mean fluxes absorbed or transmitted by trees, disregarding the spatial distribution of radiation. Some models, however, have considered the spatial variability of radiation on the floor in forest stands, but at a scale of some meters (Kuuluvainen and Pukkala, 1987; Pukkala et al, 1991).

The aim of this paper is to assess the ability of a turbid medium model to evaluate the spatial variability of the transmitted radiation below a young agroforestry plantation. For this purpose we modified the Sinoquet and Bonhomme radiative transfer model (1992) to consider three-dimensional heterogeneous canopies and to compute the spatial distribution of transmitted radiation. Tree structure and light distribution below trees were measured in an agroforestry system consisting of wild cherries (*Prunus avium*) and a pasture of *Festuca elatior*. The measurements allowed us to identify the causes of variability in transmitted radiation and to test the model.

MATERIALS AND METHODS

Field experiment

The experiment was conducted at the Cemagref (Centre d'études du machinisme agricole du génie rural des eaux et forêts) centre in Montoldre, France (46°2 N, 3°25 E). The canopy is formed by rows of wild cherries (*Prunus avium*) planted in 1990 at a density of 1 250 stems·ha^{-1}. Protection from rabbits and deer was obtained by plastic tree shelters. Trees were thinned in 1994 to 625 stems·ha^{-1}, ie, a 4 m square-planted pattern. Trees were pruned once a year for a high quality bole. The row azimuth is 31°5 E. No irrigation was supplied during the experiment. To protect the trees from *Phloeosporella padi* and aphids, chemicals were applied twice a year in June and September from planting onwards. The grass layer is mainly made up of *Festuca elatior* which is mowed twice a year in May and September.

Radiation measurements

The spatial distribution of transmitted radiation was measured in 1994 using a tracking system made up of two trolleys, each one moving on a 16 m^2 area (area #1 and area #2) delimited by four trees (fig 1). During a measurement cycle the system recorded the transmitted radiation in each area. Each trolley carried a CR10 datalogger (Campbell Scientific Ltd, Shepshed, UK) and a 4-m-long line of sensors perpendicular to the row direction mounted 1 m above the ground. A line of sensors contained 19 amorphous silicon cells (ASC; Solems, ZI Les Glaises, Palaiseau, France) spaced every 20 cm and measuring photosynthetically active radiation (PAR, 400–700 nm). The horizontality of each ASC was inspected before and after each measurement cycle. Each ASC was individually connected to the CR10 datalogger.

All PAR sensors were individually calibrated by comparison with a PAR quantum sensor (SKP 210, Skye Instruments, Llandridod Wells, Wales) although spectral responses of the two types of sensors are slightly different (Chartier et al, 1989). The tracking system moved upon two horizontal and parallel metal rails placed on the ground exactly in between two rows of wild cherries. The two trolleys were linked with an 8 m bar of metal and moved together owing to a sole motor located on one of them. Forty holes were made regularly every 10 cm on the side of one rail. An induction sensor was placed on the trolley, causing the motor to stop when a hole was detected. The motor was connected to a CR10 datalogger to make the tracking system restart after the measurements at a given location.

The average of the measurements made during 15 s was recorded for each sensor and each steady-state position of the tracking system. During one measurement cycle each trolley allowed us to record 760 (40 × 19) data on 16-m^2 area to describe the spatial distribution of light. A measurement cycle took 15 min. The datalogger memory made it possible to store the data of 16 measurement cycles.

Incident radiation in the PAR waveband was measured with an ASC placed in an open area 30 m away from the wild cherry trees. An ASC was shaded to measure the incident diffuse PAR. These sensors were connected to a third CR10 datalogger. The three dataloggers were connected together to make simultaneous measurements. Each time the trolley stopped to allow measurement, the incident radiation was measured and the average of the measurements made during 15 s was recorded. Thus, 40 diffuse to global radiation ratios (DGR) were available for each cycle of the trolleys.

Canopy structure measurements

Wild cherries show two main architectural features: leaves are inserted on twigs (up to 11 leaves per twig) and twigs are distributed all along the branches (Fournier, 1989). Therefore the three-dimensional distribution of the leaf and wood area of the eight trees surrounding the tracking system was measured as follows (fig 2): i) for each axis (stem and branches), height of the axis insertion, diameter at 2 cm from the base, length, zenith and azimuth angles, ii) for each twig, length between the twig and the insertion of the underlying axis, length of each leaf.

The area of each leaf was estimated by using a relationship between length and area. It was determined by a random sampling of 100 leaves on neighbour trees, on which length (LL, mm) and area (LA, cm^2) were measured:

$$LA = 0.0116 \times LL^{1.7263},\ r^2 = 0.94$$

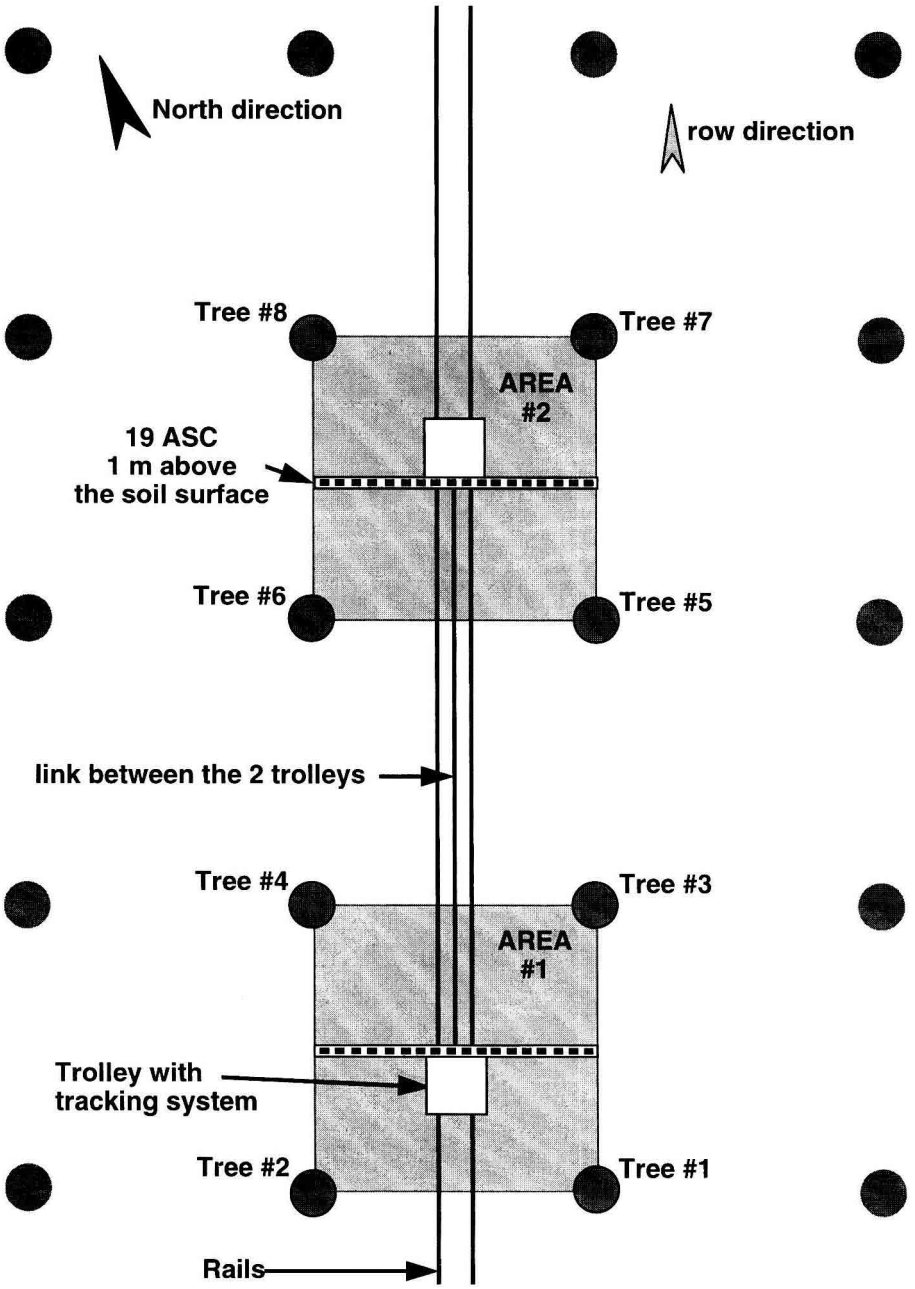

Fig 1. Scheme of the tracking system with the amorphous silicon cells on the two measurement areas.

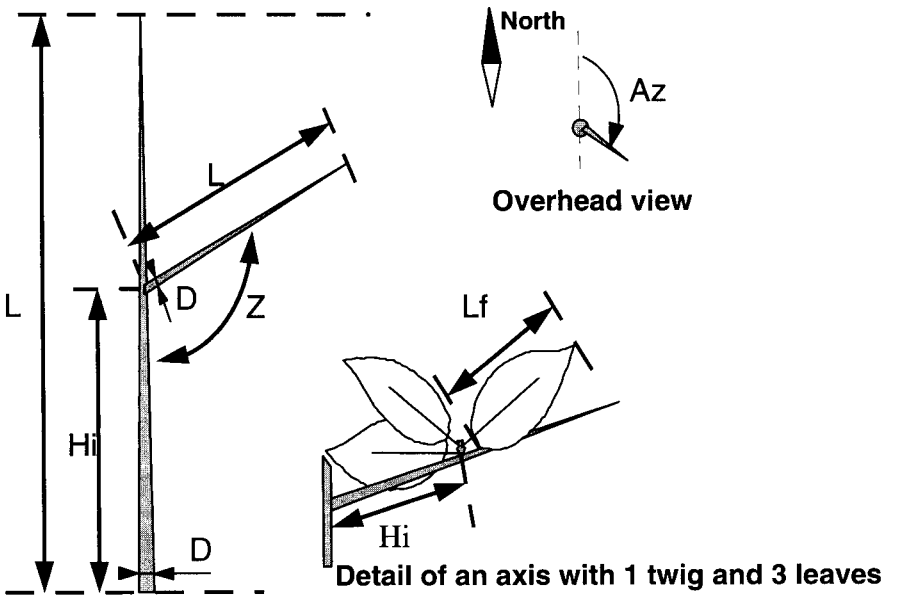

Fig 2. Scheme of the canopy structure measurements. L: length; D: diameter at 2 cm from the base; Z: zenith angle; Az: azimuth angle; Hi: height of insertion; Lf: leaf length.

The growth of wild cherry is polycyclic. The measurements given here were made during May and June 1994. During the last week of August, the same measurements were made on three main branches in two of the eight trees in order to establish the evolution of the structure. No significant difference was found between the two sets of measurements, meaning that the main growth of 1994 was accomplished at the end of May 1994 probably because of a dry summer. This was confirmed by the very small annual growth observed in the routine measurements (tree height and breast diameter) made on the plot in autumn.

Model description

The model (Sinoquet and Bonhomme, 1992) is based on the turbid medium analogy. The canopy is described as a set of elementary units divided into contiguous elementary volumes. In the original model, the space between the soil surface and the horizontal plane at the top of the canopy was divided into horizontal layers and vertical slices parallel to the row direction allowing a two-dimensional description of the canopy. In this study, the model has been extended to three-dimensional canopies, ie, three-dimensional cells are defined by the intersection of horizontal layers, vertical slices parallel to the row direction and vertical slices perpendicular to the row direction. Each cell may be empty or contain one or more plant components (leaves or woody parts). Cell content is described by the area density and inclination distribution of each component. Within a cell, area densities are assumed to be uniformly distributed, inclination distributions constant and azimuths random.

For a given direction, the path of beams regularly sampled every 1 cm is computed through the cells from simple geometrical considerations by computing the intersections between the beam path (a line) and the cell bounds (plans). Then cells visited by the beam are identified, and the path length in each cell is computed.

Beam extinction is calculated from the Beer-Nilson's law applied to each cell crossed by the

beam. The probability P_{jk} that a beam of direction Ω is intercepted by plant component j within the kth cell visited is

$$P_{jk} = \left(\prod_{l=1}^{(k-1)} \exp\left|-\sum_{i=1}^{M} \mu \cdot G_{il} \cdot a_{il} \cdot \delta_{sl}\right|\right) \cdot \left(1 - \exp\left|-\sum_{i=1}^{M} \mu \cdot G_{ik} \cdot a_{ik} \cdot \delta_{sk}\right|\right) \cdot \left(G_{jk} \cdot a_{jk} \Big/ \left|\sum_{i=1}^{M} G_{ik} \cdot a_{ik}\right|\right) \quad (1)$$

where μ is the leaf dispersion parameter (Nilson, 1971; $\mu = 1$ for a random leaf dispersion) G_{il} is the projection coefficient for the direction Ω and plant component i (see Ross, 1981), a_{il} is the area density of component i in cell l and δ_{sl} is the length of the beam path in cell l. In the standard run, leaf dispersion is assumed to be random for all the components. The three terms of Eq (1) are, respectively, i) the gap frequency above cell k, ii) the radiation intercepted by the whole plant components in the cell k, and iii) the proportion of the radiation intercepted by plant component j.

The direct component of the incident radiation is assumed to be a set of parallel beams coming from the sun position. The penumbra effect is therefore disregarded. Diffuse incident radiation is considered as a set of directional fluxes. The sky is divided into 144 solid angle sectors, ie, eight zenith angle classes and 18 azimuth classes. Hemispherical fluxes are computed by numerical integration over the whole sky.

The multidirectional origin of the scattered radiation is taken into account. The assumption is made that the radiation scattered by a plant component in the direction Ω only depends on the cosine of the angle between the normal of plant component and the exit direction Ω. Interception of scattered radiation is treated like that of incident radiation. The only difference is that beams come from the scattering zones (vegetation cells and soil surface) and their energy is defined by the scattering phase function. Interception of scattered radiation is expressed in terms of exchange coefficients $C_{A,B}$ between a source A and a receiver B of scattered radiation.

The radiative balance of the canopy is solved by using the radiosities method (Ozisik, 1981). The radiation intercepted by component j in cell k is

$$R_{jk} = R_{bjk} + R_{djk} + \sum_{l=1}^{N} \sum_{i=1}^{M} C_{il,jk} \cdot \sigma_i \cdot R_{il} + \sum_{m=1}^{Nx} C_{m,jk} \cdot \sigma_g \cdot R_{gm} \quad (2)$$

where R_{bjk} and R_{djk} are, respectively, the direct and the diffuse incident radiation intercepted by the plant component j within the cell k, $C_{il,jk} \cdot \sigma_i \cdot R_{il}$ is the scattered radiation coming from plant component i in the cell l and intercepted by the plant component j in the cell k, σ_g is the soil reflectance, R_{gm} is the radiation transmitted to the soil cell m ($m = 1,...Nx$). Equation (2) (ie, for $j = 1,...M$ and $k = 1,...N$) forms a system of linear equations where fluxes R_{jk} are the unknowns. It is solved by an iterative method.

The model has been extended to compute, for each soil cell, the transmitted radiation in the shaded and in the sunlit area separately. The shaded area (A_{sha}) is supposed to receive only the diffuse and the scattered radiation while the sunlit area (A_{sun}) receives the same diffuse and scattered radiation plus the whole direct incident radiation. The ratio of sunlit area in each soil cell corresponds to the direct radiation transmittance (Chartier, 1966) and may be written

$$A_{sun} = R_{bk} / R_{b0}$$

where R_{bk} is the direct radiation intercepted within the soil cell k and R_{b0} is the incident direct radiation above the canopy. This allowed us to estimate the standard deviation (SD) of the simulated transmitted radiation in each soil cell using the following equation

$$SD = \left(A_{sun} \cdot \left[R_{sun} - R_{sk}\right]^2 + A_{sha} \cdot \left[R_{sha} - R_{sk}\right]^2\right)^{1/2} \quad (3)$$

where R_{sk} is the mean simulated transmitted radiation in the soil cell k, R_{sun} and R_{sha} are the simulated transmitted radiations in the sunlit area and in the shaded area of the cell k, respectively.

Finally, the data obtained from the model are the mean transmitted radiation at the soil level, the transmitted radiation in each soil cell (thus, the spatial distribution of the transmitted radiation on the whole scene), the sunlit and shaded area and the standard deviation of the simulated transmitted radiation in each soil cell.

Input parameters for the model

Leaves and woody parts were considered as two components with their own optical properties. Reflectance and transmittance were measured using a spectroradiometer (Li-Cor 1800, Lincoln, NE, USA) in June 1994. Mean values of reflectance and transmittance integrated on the PAR waveband were 9 and 13 for leaves and 11 and 2 for bark, respectively. Although there were differences between measured reflectance and transmittance, a simple scattering coefficient (ie, the sum of reflectance and transmittance) was used because the model assumes bark and leaves to be lambertian diffusers.

Leaf inclination distributions were assumed to be spherical as generally reported for trees (Ross, 1981). Trunk and branch inclination distributions were, respectively, assumed to be vertical and spherical.

Sensitivity analyses of the system were made by changing the leaf inclination distribution and the leaf dispersion. Two contrasted leaf inclination distributions (ie, erectophile and planophile) were compared with the spherical leaf inclination distribution. The effect of leaf dispersion within cells was also studied by changing parameter μ in Eq (1) (Nilson, 1971): $\mu = 0.8$ to simulate a more clumped dispersion and $\mu = 1.2$ to simulate a more regular leaf dispersion.

The size of cells for the description of the canopy structure was 0.1 m according to the mean length of wild cherry leaves. A program written in C allowed us to allocate leaf and wood area in the three-dimensional cells from the canopy structure measurements. The leaf area attached to a twig was assumed to be in the cell containing the twig base. For the woody parts, the unfolded half area of the segment included in each cell was calculated assuming that woody parts were cylinders.

The elementary unit used for the simulation was a frame of 8 m × 8 m, ie, the soil surface occupied by four trees. The elementary unit included 236 800 cells: 1 280 (area #1) and 1 430 (area #2) cells contained leaves or woody parts. The whole canopy was assumed to be made up of replicates of the elementary unit placed side by side.

As DGR was not constant during the 15 min necessary for the whole area measurement (fig 3), two simulations were made for each simulated cycle: one with DGR = 0 and one with DGR = 1. The transmitted radiation for each trolley stop, and therefore for each measurement line, was computed by summing the two simulated transmitted radiation weighted by DGR_k, which was the diffuse to global ratio corresponding to the recording position of the cell k:

$$R_{sk} = R_{sk}(1)\cdot DGR_k + R_{sk}(0)\cdot(1 - DGR_k) \quad (4)$$

where R_{sk} was the transmitted radiation in the cell k, $R_{sk}(1)$ the transmitted radiation computed with DGR = 1 in the cell k, $R_{sk}(0)$ the transmitted radiation computed with DGR = 0 in the cell k.

Data analysis

The behaviour of the model was tested by comparing simulated and measured values. Eight cycles were chosen to test the model. Each cycle was made of 760 values of transmitted radiation for each area. The eight cycles were made in various conditions of incident radiation (fig 3) to scan different sun positions, different DGR and different variations of the incident radiation during the cycle (table I). The incident radiation was constant during cycle 2 (low DGR 0.33); during the other cycles, incident radiation showed more or less pronounced variations and the mean DGR was between 0.34 and 0.88. Sun height was always more than 39° to limit shading by trees of neighbour rows, the geometrical structure of which was not described. This allowed small radiation fluxes coming from elevations lower than 39° (ie, diffuse radiation in all cycles and direct radiation in cycle 8).

The data were analysed in three ways. First the average transmitted radiation was computed on a simulated and measured area. Second, the study focused on the radiation distribution under the trees. The spatial pattern of radiation distribution was disregarded, ie, the analysis was made on simulated and measured data arranged independently in ascending order. Third, the spatial pattern was taken into account by considering paired data, ie, values taken at the same location below the trees. For the second analysis, as the values were arranged in ascending order, we could not make a regression analysis and the quality of the model was assessed only by the mean square error of prediction (MSEP):

$$MSEP = \sum_{m=1}^{N} (R_{mk} - R_{sk})^2 / N$$

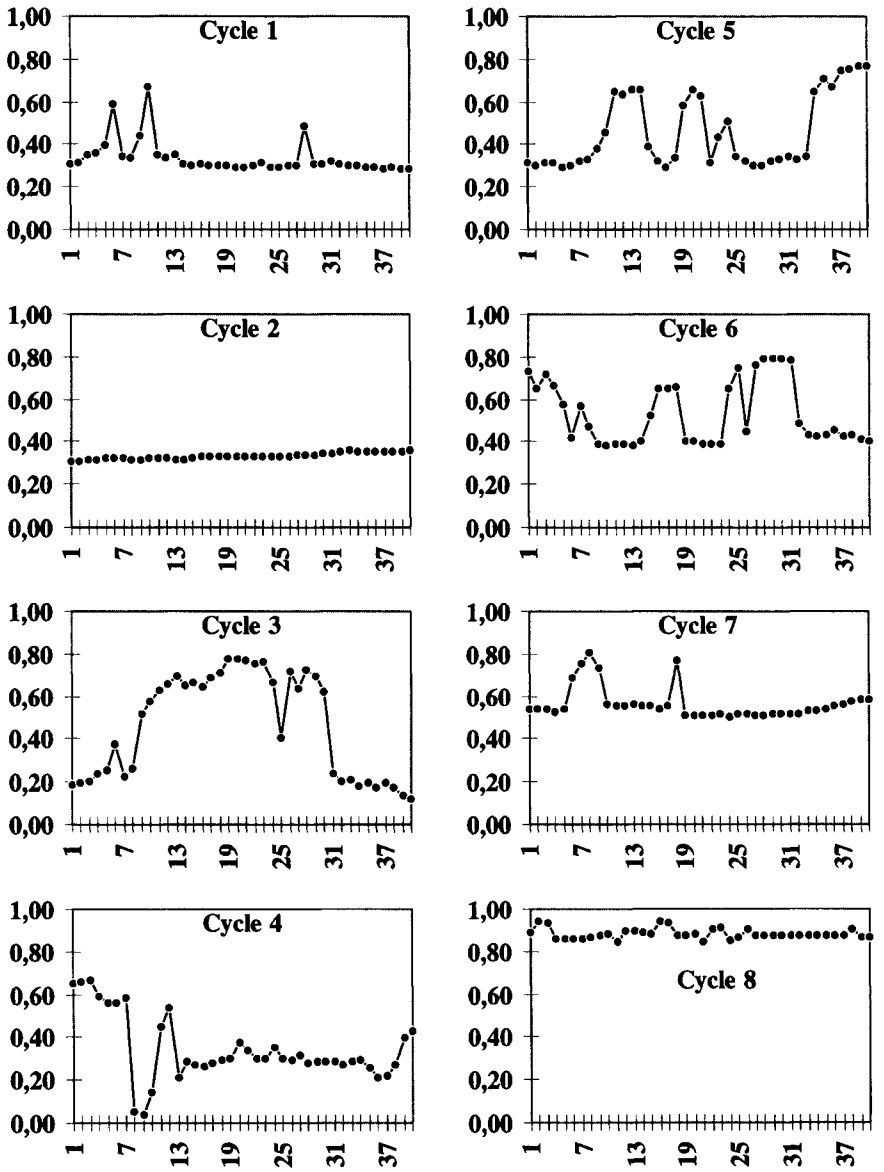

Fig 3. Evolution of the diffuse to global radiation ratio (DGR) during the eight cycles chosen for the analysis.

where R_{mk} and R_{sk} were, respectively, the relative transmitted radiation measured and simulated in cell k and Nx the number of soil cells (760 for the whole area). For the third analysis, regression analysis and mean square error of prediction were calculated. The same analysis was repeated with the mean radiation transmitted onto contiguous and non-overlapping areas corre-

Table I. Characteristics of the above canopy radiation field for the eight cycles studied.

Cycle no	*Calendar day*	*True solar time (TST)*	*Sun height*	*Sun azimuth /tree row*	*Mean DGR*	R_i *min*	R_i *max*
1	163	08h21	40.65	–113	0.35	480.43	980.35
2	163	09h21	50.65	–99.35	0.33	1 101.42	1 166.38
3	166	10h54	63.57	–66.98	0.46	386.12	1 505.65
4	166	11h54	67.06	–34.65	0.34	507.00	1 501.51
5	165	12h54	64.51	–1.09	0.46	389.96	1 482.04
6	165	13h54	57.41	23.55	0.53	382.11	1 391.73
7	165	14h54	48.11	40.51	0.56	331.41	1 165.68
8	250	08h14	27.41	–100.2	0.88	54.48	124.77

Each cycle lasted 15 min. True solar time, sun height (°), sun azimuth (°) in relation to tree row are taken exactly at the middle of the cycle. The diffuse to global radiation ratio (DGR) is an average computed with the 40 values recorded during each cycle. $R_i$max and $R_i$min are, respectively, the maximal and minimal incident radiation ($\mu mol \cdot m^{-2} \cdot s^{-1}$) recorded during each cycle.

sponding to a group of n sensors at the same location on the measured and simulated patterns.

RESULTS

Canopy structure

Twig length was very short (< 2 cm) and a mean of 4.5 leaves was attached on a twig. An average distance of 3.3 cm separated two twigs on the same axis. As the phyllotaxy of wild cherry is 2/5, the distance between two aligned twigs on the same axis was 16.5 cm. The mean lengths of petiole and lamina were, respectively, 15 and 56 mm. Accordingly, the distribution of leaf area along an axis was discontinuous and showed clumped behaviour. Fournier (1989) also noted this pattern of leaf area distribution characterized by a muff of twigs sheathering the axis. Relationships between axis diameter at 2 cm from the base (D, mm), total leaf area of the axis (TLA, m^2), axis length (L, mm) and number of twigs on the axis (NT) were calculated including all branching orders except trunks. The relationships can be used to simplify future canopy measurements on the wild cherries

$$NT = 0.00004 \times L^2 + 0.0032 \times L \quad r^2 = 0.90$$

$$L = 2.7304 \times D^2 + 84.798 \times D \quad r^2 = 0.87$$

$$TLA = 0.0043 \times D^2 - 0.0039 \times D \quad r^2 = 0.91$$

Table II gives canopy structure parameters at the tree scale.

Crown width was estimated from the vertical projection of the vegetation three-dimensional cells onto the soil surface. For similar total heights (4.3–5 m) and crown heights (2–2.8 m), differences between the eight trees were important in terms of crown width (1.4–2.9 m) and total leaf area (1.8–8.6 m^2). Figure 4 shows vertical leaf area profiles of two contrasting trees and the ground cover of the two scenes. The number of three-dimensional cells with leaves or branches fluctuated from 242 for tree #4 to 471 for tree #8 with an average of 350 cells.

Distribution of measured radiation below the trees

Examples of radiation distribution measured below the trees are showed in figure 5. On cycles 1–7, 70–90% of the understorey

Table II. Canopy structure parameters as measured on June 1994.

Tree no	*Height (m)*	*Total leaf area (m^2)*	*Crown width (m)*	*Crown height (m)*
1	4.8	8.2	2.9	2.8
2	4.7	4.6	2.1	2.7
3	4.5	5.3	2.1	2.4
4	4.6	1.8	1.4	2.2
5	4.7	7.2	2.5	2.6
6	4.8	5.4	2.2	2.7
7	4.3	3.4	1.6	2.
8	5	8.6	2.1	2.8

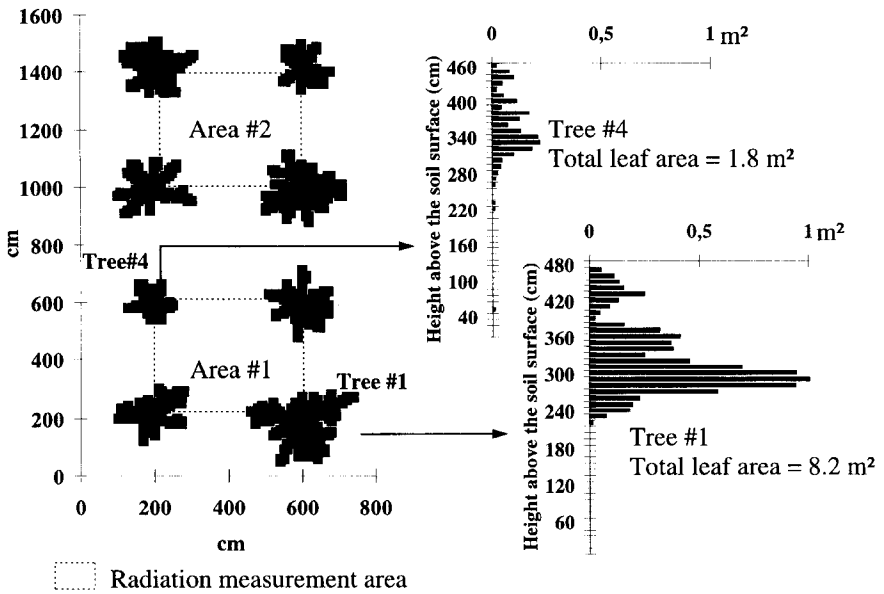

Fig 4. Vertical projection of the 10 cm × 10 cm cells constituting the two simulation scenes and vertical leaf area profiles of two contrasting trees (#1 and #4).

received more than 90% of the incident radiation. The small differences observed in the 90–100% radiation class between the two areas may be related to the characteristics of the tree responsible for shadow on the measurement area: for instance, on cycles 1 and 2, area #1 was mainly shaded by tree #3, which was larger than tree #7, which shaded area #2; on cycles 3–7, the two areas were shaded by tree #2 and tree #6, which had similar development (table II, fig 4). The lowest values of transmitted radiation on cycles 1–7 (DGR < 0.6) were about 30% and similar for the two areas. For the two areas and the seven cycles, radiation distribution between 30 and 90% was not signif-

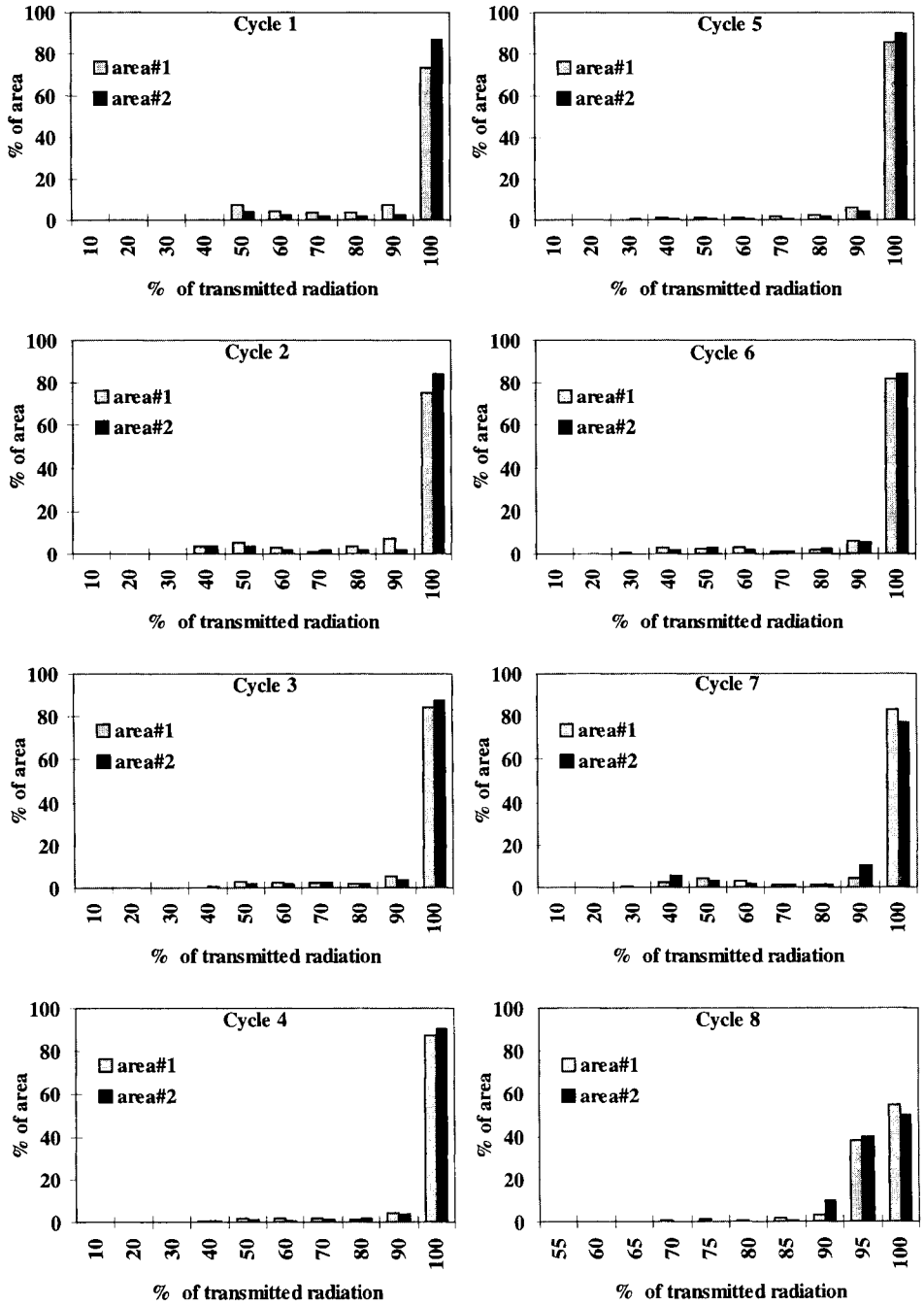

Fig 5. Distribution of the measured transmitted radiation for the eight cycles on the two areas.

icantly different from a uniform distribution (χ^2 test, $P < 0.05$). On cycle 8 (DGR > 0.8), transmitted radiation rarely fell below 85% (fig 5). Most of the understorey received more than 90% of the incident radiation.

Model validation

Comparison between measured and simulated values of transmitted radiation

Mean simulated and measured transmitted radiation are presented in table III. Mean measured values were always greater than 80% of the incident radiation whatever the sun position or DGR. Mean values were also quite equal on a 16 m^2 area (area between four trees) whatever the sun position or DGR: the difference between measurement and simulation values reached a maximum of 3% (eg, cycle 3), which corresponds to a maximum error of 45 $\mu mol \cdot m^{-2} \cdot s^{-1}$.

Comparisons between distributions of measured and simulated transmitted radiation are presented as quantile–quantile plots (Q-Q plots) in figure 6. Using Q–Q plots makes it possible to compare the measured and simulated fractions of understorey receiving a given range of transmitted radiation: the range is the quantile value equal to 5% in this analysis. On the whole, measurements and simulations are in agreement. On cycles 1–7 transmitted radiation above 90% of the incident radiation is accurately simulated because i) it corresponds to sunlit areas, ii) the main part of the soil surface area is sunlit, and iii) the model is able to discriminate between the sunlit and the shaded area. Deviations in lower transmitted values may be either positive or negative (fig 6, cycles 1–7). Cycles 3 and 4 show a strong deviation when the measured transmitted radiation is less than 40% of the incident radiation; in that case, the square-root of MSEP reaches 24% on area #1 and 19% on area #2 (cycle 4). Only five points are involved in this deviation; therefore, only 0.6% of the measurement area is affected. On cycle 8 the model slightly underestimates radiation transmission. The square-root of MSEP is 7%, which is a small value when referred to the level of the incident radiation (55–125 $\mu mol.m^{-2} \cdot s^{-1}$). In areas submitted to the tree shadow (transmitted radiation < 90%) discrepancies may be more important: square-root of MSEP is up to 9%. However with regard to the level of the incident radiation the absolute deviation between the measurement and the simulation reaches a maximum of 135 $\mu mol \cdot m^{-2} \cdot s^{-1}$.

Maps in figure 7 show examples of the spatial pattern of simulated and measured transmitted radiation. On cycles 1–7, the general shape of the shade is quite similar for simulated and measured transmitted radiation. The shaded points are more or less at the same location on the two maps although the measured shadow is more diffuse. On cycle 8 (characterized by a high mean DGR) neither the measured map nor the simulated one shows simple spatial structure. This is

Table III. Comparison between mean measured and simulated transmitted radiation (% of incident radiation).

Cycle	*1*		*2*		*3*		*4*		*5*		*6*		*7*		*8*	
Area #	*#1*	*#2*	*#1*	*#2*	*#1*	*#2*	*#1*	*#2*	*#1*	*#2*	*#1*	*#2*	*#1*	*#2*	*#1*	*#2*
Measured	88	92	89	91	92	93	92	94	92	93	90	91	89	88	93	92
Simulated	89	89	90	91	89	90	92	92	92	91	90	90	90	89	90	89

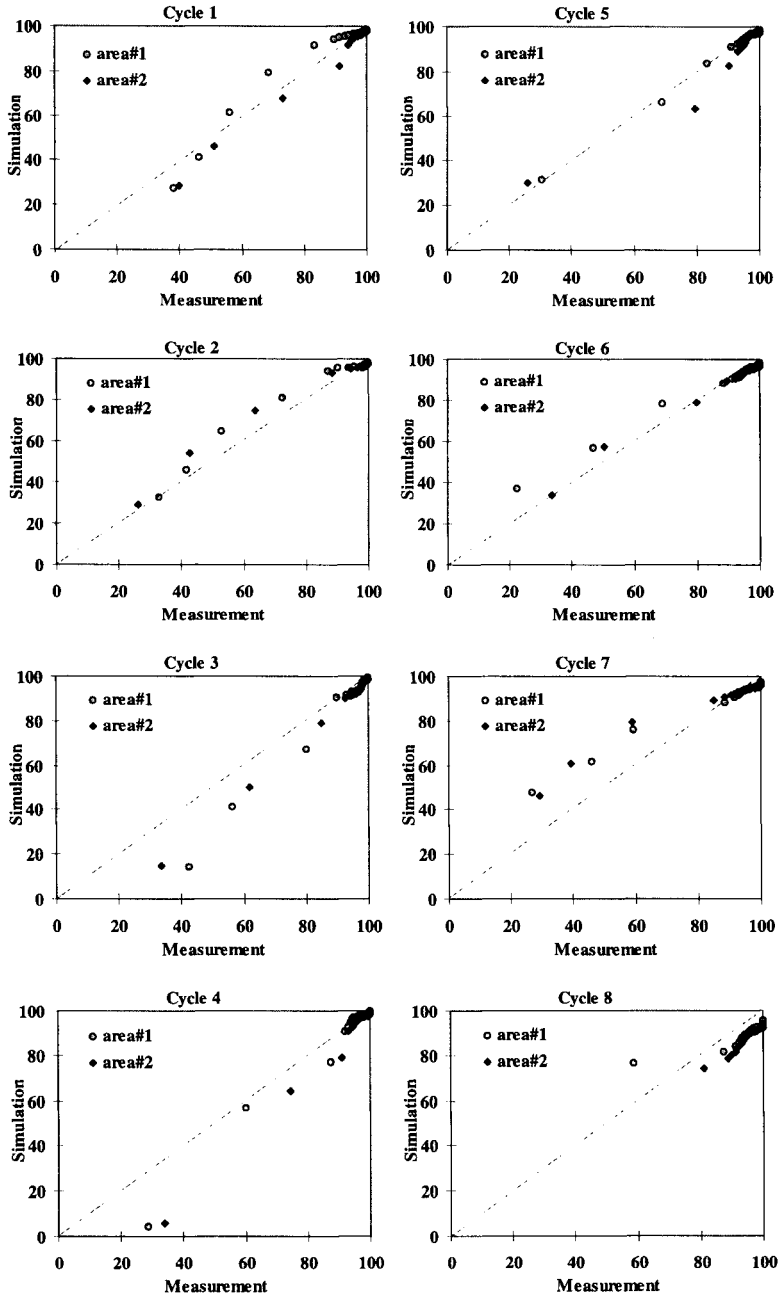

Fig 6. Quantile–quantile plots of measured and simulated transmitted photosynthetically active radiation (PAR) (% of incident radiation) for the eight cycles on the two areas. The quantile value is 5%.

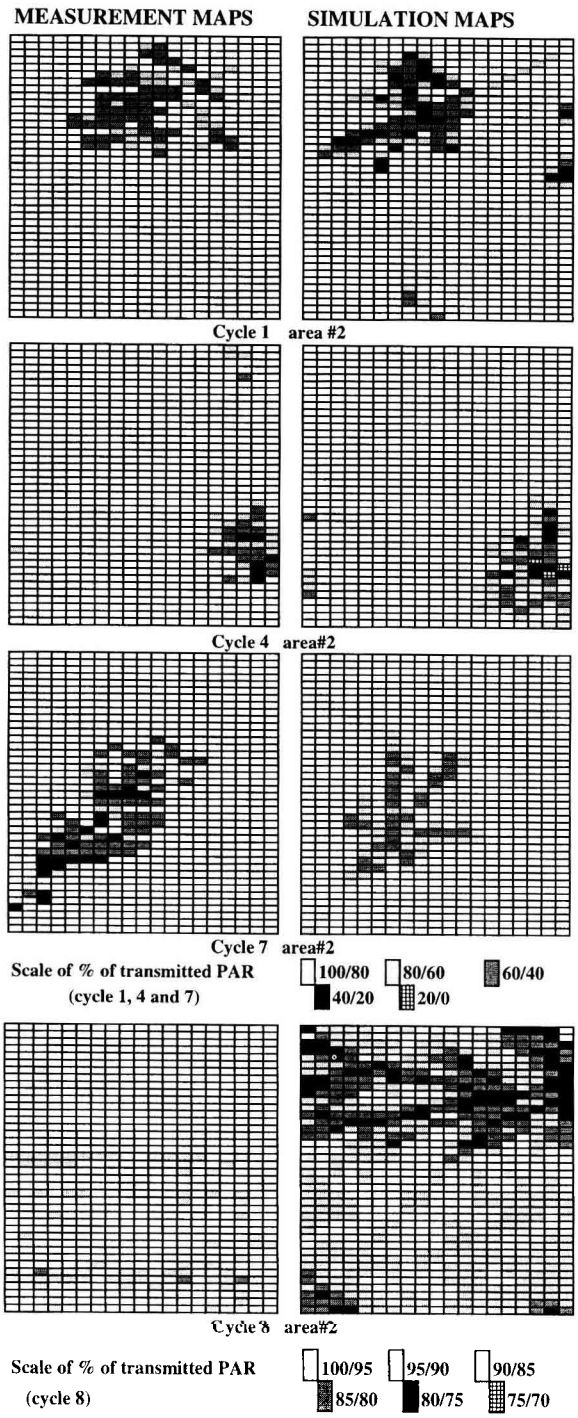

Fig 7. Maps of measured and simulated transmitted radiation for four cycles on area #2. PAR: photosynthetically active radiation.

probably because, unlike in the sunny sky conditions (cycles 1–7), several trees contributed in the same proportion to radiation interception.

Considering the spatial pattern of radiation distribution the model poorly grasps the variability of the transmitted radiation at the scale of the sensor (n = 1): regression analysis gives r^2 coefficients between 0 and 0.39. The point to point comparison between the measurement and the simulation (fig 8) emphasizes that the maximum deviation occurs when points are sunlit in the measurement or the simulation and shaded in the corresponding measured or simulated area. Thus, the maximum error occurs on the edges of the tree shadow.

Increasing the area of comparison (by averaging transmitted radiation on n sensors) improves the relationships. The most significant improvement is shown when the area increases from 0.02 m^2 (n = 1) to 0.08 m^2 (n = 4). For several cycles (cycle 2 area #1, cycle 3 area #1, cycle 6 area #2 and cycle 7 area #1) measured and computed distributions agree when 16 sensors are grouped ($r^2 > 0.80$ and square-root of MSEP = 4–6%): thus, spatial variability is correctly simulated from a 0.6 m × 0.3 m area. However, for the other cycles, the r^2 coefficient never reaches 0.75 even if transmitted radiation is averaged on 16 sensors. For the high DGR cycle, the r^2 coefficient is 0 whatever the integration area.

The same analysis is made on the shaded area only. The shaded area is defined as the set of points such that measured or simulated transmitted radiation is less than 90% of the incident radiation. At the scale of the

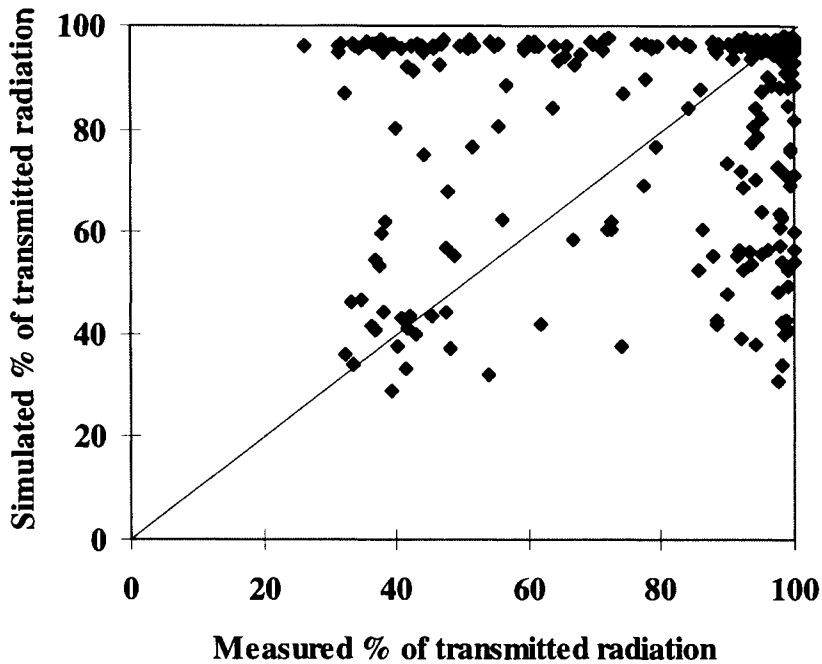

Fig 8. Point-to-point comparison between simulated and measured transmitted radiation distribution on cycle 2 area #2.

sensor the square-root of MSEP on the shaded area reaches 32% (cycle 2 area #2) even though the maximum square-root of MSEP in the total area is 18%. This difference is mainly due to the large fraction of the sunlit area (up to 87% of the area) which is well simulated in the total area leading to a decrease of square-root of MSEP. The regression coefficient showed that the model could not give the variability of the transmitted radiation in the shaded area at the scale of the sensor. Increasing the area of comparison improves the relationship: the regression coefficients in the shaded area are close to those in the total area in 75% of the cycles studied (cycles 3–7) when $n = 16$.

Comparisons between measurement and simulation using the absolute transmitted radiation ($\mu mol \cdot m^2 \cdot s^{-1}$) are computed from the relative simulated transmitted radiation and the incident measured radiation. Because the absolute value integrates variations in the incident radiation during the measurement cycle, the r^2 coefficients are better. Of particular interest is cycle 8: the r^2 coefficient reaches 0.96 at the sensor scale because the incident radiation varies from 1 to 2.3 (54–124 $\mu mol \cdot m^2 \cdot s^{-1}$) even though the r^2 coefficient never reaches 0.01 in the analysis on the relative values. Integrating the transmitted radiation over larger areas improves the relationship and the r^2 coefficient is over 0.75 for cycles 3–7 from $n = 4$. The square-root of MSEP is between 7.62 (cycle 8 area #1) and 361 $\mu mol \cdot m^2 \cdot s^{-1}$ (cycle 2 area #2) at the sensor scale which corresponds, respectively, to 6 and 31% of the maximum incident radiation of the cycle. When integrating on 16 sensors (0.32 m^2) the square-root of MSEP is between 6.91 (cycle 8 area #1) and 129 $\mu mol \cdot m^2 \cdot s^{-1}$ (cycle 2 area #2) which corresponds, respectively, to 5 and 11% of the maximum incident radiation of the cycle.

Sensitivity analysis

The comparison between the simulations made with different leaf inclination distributions (spherical, erectophile and planophile) allowed us to test the importance of this parameter in the Sinoquet and Bonhomme model. The square-root of MSEP is less than 2%, the regression slope is not significantly different from 1 and the r^2 coefficient is 0.99 whatever the sun position or the DGR. This shows that the model is not sensitive to leaf inclination distribution. Therefore, the spherical distribution can be used in the description of the tree structure without increasing simulation errors.

A leaf dispersion parameter was introduced in each cell containing leaves to test the sensitivity of the model to the dispersion of the foliage elements. The square-root of MSEP between simulations with random or non-random foliages is less than 1.5% whatever the sun position or the DGR; regression slope and r^2 coefficients show very small differences in transmitted radiation between a random and clumped canopy ($\mu = 0.8$) or between a random or more regular canopy ($\mu = 1.2$). Therefore, the model is not sensitive to the dispersion of the leaf area within the cells.

Standard deviation

Examples of maps of standard deviation computed for each cell are shown in figure 9.

Standard deviation between 20 and 50% are only present in the shaded area. The standard deviation in the shaded area does not show simple spatial structure. On cycle 8 the standard deviation never reaches 20%. In the afternoon, the maximum of standard deviation on the simulated area decreases with sun height. The maximum standard deviation of the transmitted radiation simulated in a cell is 50% whatever the sun posi-

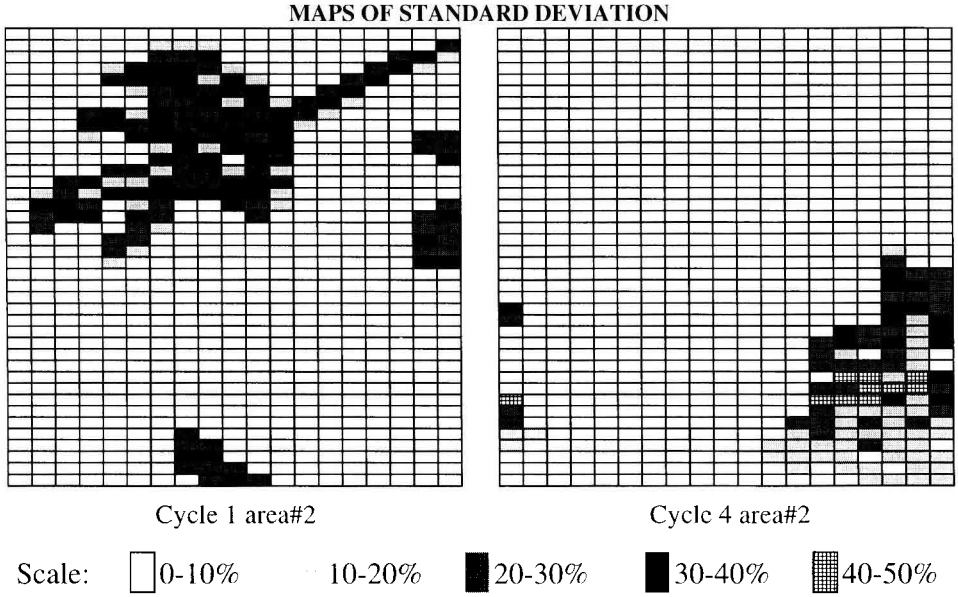

Fig 9. Maps of standard deviation of simulated transmitted radiation for two cycles on area #2.

tion or DGR. Accordingly, it appears that the transmitted radiation in the simulated shaded area is subject to high variation coefficient (standard deviation divided by the mean simulated transmitted radiation) up to 56%, detrimental to the accuracy of the model.

DISCUSSION

Variability in radiation available to the understorey

There are at least two main reasons for spatial variability of radiation available to the understorey. First, trees may show large morphological differences. In our experiment leaf area of trees varied from 1.8 to 8.2 m^2 while crown width of the largest trees was twice that of the smallest ones. Moreover, not only total leaf area but also its spatial distribution within the crown influences transmitted radiation (Oker-Blom, 1986). The shade of trees with the same total leaf area but with different distribution could be different. On the other hand, irradiance distribution in the shaded understorey (ie, transmitted radiation < 0.9) is uniform whatever the tree (χ^2 test, $P < 0.05$).

Second, radiation variability also exists at a smaller scale, which defines the fine spatial pattern of light transmission. In the case of a clear sky, points at the understorey level may have been exposed to direct radiation or not according to the gaps within the tree crown, depending on the location of the phytoelements. Irradiance at a given point within or below a canopy may be treated as a random variable (eg, Oker-Blom, 1986) while the radiation measurement corresponds to a particular event associated with the random variable. The computation of the standard deviation shows that the variability of

the simulation at the local scale is very high (up to 50%) in the case of low DGR (ie, clear sky). On a more cloudy cycle (cycle 8), the spatial pattern of transmitted radiation does not show any identified structure, as previously reported by Tang and Washitani (1995) in a *Miscanthus sinensis* canopy. However, the small range of values of transmittance associated with lower incident radiation leads to small variations in the amounts of PAR received by the understorey.

Modelling spatial variability of transmitted radiation

From the previous section, it appears that radiation distribution below young trees shows large variations for clear sky conditions. In that case, irradiance distribution is characterized by: i) a high fraction of area where transmitted radiation is greater than 90% of the incident radiation, ii) a uniform distribution of the lower irradiances and iii) a minimum value of transmitted radiation. The spatial pattern of radiation distribution is partly defined by the shadow cast by the trees. Therefore, a light model aimed at simulating spatial variability in such a tree–grass system should be able to provide these features of the radiation field above the understorey.

The Sinoquet and Bonhomme model is able to simulate the mean transmitted radiation on a 16 m^2 area with a maximum error of 3%. The model correctly simulates the relative sunlit area and the relative shaded area and the irradiance frequency in the class 90–100% and the uniform distribution of radiation in the lower classes. However, the lower bound of the radiation distribution is inaccurately simulated in 70% of the studied cases: when measured transmitted radiation is less than 40% of the incident radiation, the model often under- or overestimates the transmitted radiation. Therefore, if the shaded area increases with larger trees, the ability of the model in simulating the irradiance distribution would probably decrease.

The spatial distribution of the transmitted radiation is poorly captured by the model. The shaded area is globally well located in the simulated area but the edge of the shaded area is subject to a large variation and is sharper in the simulation. This may be due i) to the wind effect on leaves leading to a measured transmitted radiation (averaging over 15 s for each sensor) different from the simulated one, ii) to small errors on the tree structure measurements or iii) to the penumbra effect, which is not considered in the model. First, the leaf movements due to the wind tend to homogenize the transmitted radiation at the scale of the sensor. Therefore this should increase the minimum of transmitted radiation measured under the trees and blur the edge of the shaded area. Second, small errors in the canopy structure measurement can lead to errors in locating leaf area in three-dimensional cells, and then to errors in computing beam extinction, especially at a small space scale. Third, the penumbra effect is not taken into account in the Sinoquet and Bonhomme model because it involves larger computation time and memory: in this study, 35 h were necessary to run the model on one area (16 m^2) on a SPARC20 work station with 64 MoRAM. Horn (1971) showed that a leaf of diameter d involves a total penumbra for a distance of about 108 d. In the case of the young wild cherry, the length of a leaf is 56 mm consequently the total penumbra occurs at 6 m from the leaf. In this study, the maximum distance between a leaf and the sensors is 4.2 m so the sensors are only in partial penumbra. However, the penumbra effect also leads to homogenization of the transmitted radiation and then to an increase in the minimum transmitted radiation measured at the scale of the sensor.

The deviations between measurement and simulation by the Sinoquet and Bonhomme model are important in the shaded

area. The transmitted radiation in a particular cell in the shaded area cannot be accurately estimated by the model. The accuracy is improved when the transmitted radiation is averaged on a square including several sensors. This may be due to the hypothesis used in the model including the canopy description in three-dimensional cells: i) the leaf area density is uniformly distributed within the cell and ii) within a cell the inclination distribution is constant and the azimuth random. First, wild cherries have a characteristic structure with leaves attached to twigs creating clusters of leaves distributed along the branches. The size of the three-dimensional cells has been chosen to fit the cluster, therefore the canopy structure description used in the model should correctly account for the actual leaf dispersion within the crown. An excessive clumping could be in allocating the total leaf area of a twig only to the cell containing the twig base. However, the sensitivity test made on the Sinoquet and Bonhomme model using Nilson's approach (1971) to account for a non-random leaf dispersion suggests that the excessive clumping does not significantly affect the simulated transmitted radiation. Second, no experimental data confirm the assumption of a uniform leaf orientation. Campbell (1986) and Goudriaan (1988), among many others, have noted that the extinction coefficient used in the Beer–Lambert's law is not very sensitive to the inclination distribution. The sensivity test made with the Sinoquet and Bonhomme model confirms that the transmitted radiation is not significantly affected by changing the inclination distribution.

Finally, the variation coefficient of the transmitted radiation simulated in a cell reaches 56% of the incident radiation, which corresponds to the level of the deviation between measured and simulated transmitted radiation (square-root of MSEP divided by the mean transmitted radiation) in the shaded area. Thus, the comparison between measurement and simulation cannot give better results at the scale of the sensor than is consistent with the above results. The greatest accuracy is reached when $n = 4$ or $n = 9$ leading to a minimal surface of prediction from 0.08 to 0.18 m^2.

A way to improve the simulation of radiation variability may be to use models based on an explicit description of the canopy structure, ie, where the location, orientation and shape of the vegetation elements are individually taken into account and the radiation field is computed from raytracing techniques (Dauzat and Hautecoeur, 1991; Goel et al, 1991). But these types of models are probably difficult to apply to large vegetation scenes because of requirements in computing time and memory. Moreover, these models require a detailed canopy structure description involving tedious field measurements: in this study, 4 man-months were necessary to describe the eight young trees at the leaf level.

More simple models could be used at best to simulate the tree shadow and possibly the radiation distribution in the shaded area without considering the spatial pattern. Cohen and Fuchs (1987) considered an orchard canopy as divided into aggregates corresponding to groups of leaves. Norman and Jarvis (1975) proposed a grouping model applied to a Sitka spruce forest in which shoots are randomly located within the confine of a whorl and whorls randomly located in the horizontal plane. Oker-Blom and Kellomaki (1983) also used a two-level grouping approach in a Scots pine stand: clumping of needles in shoots and shoots in the tree crown. Such methods could be applied to the wild cherry trees because twigs are distributed in cylindrical volumes around the branches. This will allow easier canopy structure measurements at the branch level (length, azimuth and zenith angles, diameter of the axes) combined with allometric relationships. This has to be tested for model comparison with the Sinoquet and Bonhomme model.

CONCLUSION

Large variations in radiation distribution below young agroforestry trees only occurred in clear sky conditions. Thus, irradiance variability was mostly due to the high fraction of sunlit area while lower irradiances were uniformly distributed to a lower bound. The shadow cast by the trees partly defined the spatial pattern of radiation distribution whereas the fine spatial pattern within the tree shadow was random.

The Sinoquet and Bonhomme model correctly simulated the mean transmitted radiation as well as the irradiance distribution below the young trees; however, it was unable to simulate the fine spatial pattern, as probably most of the models in the literature, because of the stochastic nature of transmitted radiation. This suggests that the temporal distribution of the transmitted radiation, which results from the successive states of the spatial distribution, also cannot be simulated. Consequences for plant growth modelling may be very important when ecophysiological processes are related to light duration (eg, photomorphogenesis: Varlet-Grancher and Gautier, 1995; the effect of the sunfleck fluctuations on the understorey photosynthesis: Pearcy et al, 1990).

In fact, most of the primary production models only need the mean value of transmitted radiation (eg, Monteith's growth analysis, 1972). However, the linkage between the photosynthesis process and radiation interception by the understorey could be improved by using the radiation distribution rather than the mean value of the transmitted radiation. Simplifications have now to be tested to reduce the number of input parameters, particularly with regard to the canopy structure description.

ACKNOWLEDGMENTS

This work was partly supported by the AIR program of the EEC (AIR3-CT 920134).

REFERENCES

Baldocchi DD, Hutchison BA (1986) On estimating canopy photosynthesis and stomatal conductance in a deciduous forest with clumped foliage. *Tree Physiol* 2, 155-168

Campbell GS (1986) Extinction coefficient for radiation in plant canopies calculated using an ellipsoidal inclination angle distribution. *Agric For Meteorol* 36, 317-321

Chartier M, Bonchrétien P, Allirand JM, Gosse G (1989) Utilisation des cellules au silicium amorphe pour la mesure du rayonnement photosynthétiquement actif (400–700 nm). *agronomie* 9, 281-284

Chartier P (1966) Etude du microclimat lumineux dans la végétation. *Ann Agron* 17, 571-602

Chazdon RL (1988) Sunflecks and their importance to forest understorey plants. *Adv Ecol Res* 18, 1-63

Cohen S, Fuchs M (1987) The distribution of leaf area, radiation, photosynthesis and transpiration in a Shamouti orange hedgerow orchard. I. Leaf area and radiation. *Agric For Meteorol* 40, 123-144

Dauzat J, Hautecoeur O (1991) Simulations des transferts radiatifs sur maquettes informatiques de couverts végétaux. Proc of the 5th International Colloquium - Physical measurements and signatures in remote sensing, Courchevel, France, 415-418

Fournier D (1989) Modélisation de la croissance et de l'architecture du Merisier (*Prunus avium* L). Application à une sylviculture à large espacement. Mémoire de DAA, ENSA-Montpellier, France

Goel NS, Rozehnal I, Thompson R (1991) A computer graphics based model for scattering from objects of arbitrary shapes in the optical region. *Remote Sensing Environ* 36, 73-104

Goudriaan J (1988) The bare bones of leaf-angle distribution in radiation models for canopy photosynthesis and energy exchange. *Agric For Meteorol* 43, 155-169

Horn HS (1971) *The Adaptative Geometry of Trees*. Princeton University Press, Princeton, NJ, USA, 145 p

Jackson JE (1983) Light climate and crop-tree mixtures. In: *Plant research and agroforestry* (PA Huxley ed), ICRAF, Nairobi, Africa, 365-377

Jarvis PG (1991) Preface. In: *Agroforestry: Principles and Practice* (PG Jarvis, ed), Elsevier, Amsterdam, The Netherlands, 356

Kimes DS, Kirchner JA (1982) Radiative transfer model for heterogeneous 3-D scenes. *Applied Optics* 21, 4119-4129

Kuuluvainen T, Pukkala T (1987) Effect of crown shape and tree distribution on the spatial distribution of shade. *Agric For Meteorol* 40, 215-231

McMurtrie R, Wolf L (1983) A model of competition between trees and grass for radiation, water and nutrients. *Ann Bot* 52, 449-458

Monteith JL (1972) Solar radiation and productivity in tropical ecosystems. *J Appl Ecol* 9, 747-766

Myneni RB, Ross J, Asrar G (1989) A review on the theory of photon transport in leaf canopies. *Agric For Meteorol* 45, 1-153

Nilson T (1971) A theoretical analysis of the frequency of gaps in plant stands. *Agric For Meteorol* 8, 25-38

Norman JM, Jarvis PG (1975) Photosynthesis in Sitka spruce (*Picea sitchensis* (Bong) Carr). V-Radiation penetration theory and a test case. *J Appl Ecol* 12, 839-878

Norman JM, Welles JM (1983) Radiative transfer in an array of canopies. *Agron J* 75, 481-488

Nygren P (1993) Un modelo de los patrones de sombra de arboles manejados con podas periodicas en sistemas agroforestales. *Pesq Agropec Bras* 28, 177-188

Oker-Blom P (1986) Photosynthetic radiation regime and canopy structure in modelled forest stands. *Acta For Fenn* 197, 1-44

Oker-Blom P, Kellomaki S (1983) Effect of grouping of foliage on the within-stand and within-crown light regime: comparison of random and grouping canopy models. *Agric For Meteorol* 28, 143-155

Ozisik NM (1981) *Radiative Transfer*. John Wiley & Sons, New York, NY, USA, 579 p

Pearcy RW, Roden JS, Gamon JA (1990) Sunfleck dynamics in relation to canopy structure in a soybean (*Glycine max* (L.) Merr.) canopy. *Agric For Meteorol* 52, 359-372

Pukkala T, Becker P, Kuuluvainen T, Oker-Blom P (1991) Predicting spatial distribution of direct radiation below forest canopies. *Agric For Meteorol* 55, 295-307

Quesada F, Somarriba E, Vargas E (1989) Simulation of tree shadows in agroforestry systems. In: *Meteorology and Agroforestry* (WE Reifsnyder, TO Darnhofer, eds), ICRAF, Nairobi, Kenya, Africa, 141-156

Reid R, Ferguson S (1992) Development and validation of a simple approach to modelling tree shading in agroforestry systems. *Agrofor Syst* 20, 243-252

Ross J (1981) *The Radiation Regime and Architecture of Plant Stands*. Dr Junk Publishers, The Hague, the Netherlands, 391 p

Sinoquet H, Bonhomme R (1992) Modeling radiative transfer in mixed and row intercropping systems. *Agric For Meteorol* 62, 219-240

Tang YH, Washitani I (1995) Characteristics of small-scale heterogeneity in light availability within a Miscanthus sinensis canopy. *Ecol Res* 10, 189-197

Tournebize R, Sinoquet H (1995) Light interception and partitioning in a shrub/grass mixture. *Agric For Meteorol* 72, 277-294

Varlet-Grancher C, Gautier H (1995) Plant morphogenetic responses to light quality and consequences for intercropping. In: *Ecophysiology of Tropical Intercropping* (H Sinoquet, P Cruz, eds), INRA Editions, Paris, France, 231-256

Wang YP, Jarvis PG (1990) Influence of crown structural properties on PAR absorption, photosynthesis, and transpiration in Sitka spruce: application of a model (MAESTRO). *Tree Physiol* 7, 297-316